arXiv:2509.22652v2 [cs.RO] 11 Mar 2026

Pixel Motion Diffusion is What We Need for Robot Control

E-Ro Nguyen* Yichi Zhang* Kanchana Ranasinghe Xiang Li Michael S. Ryoo
Stony Brook University
eronguyen@cs.stonybrook.edu
eronguyen.github.io/DAWN

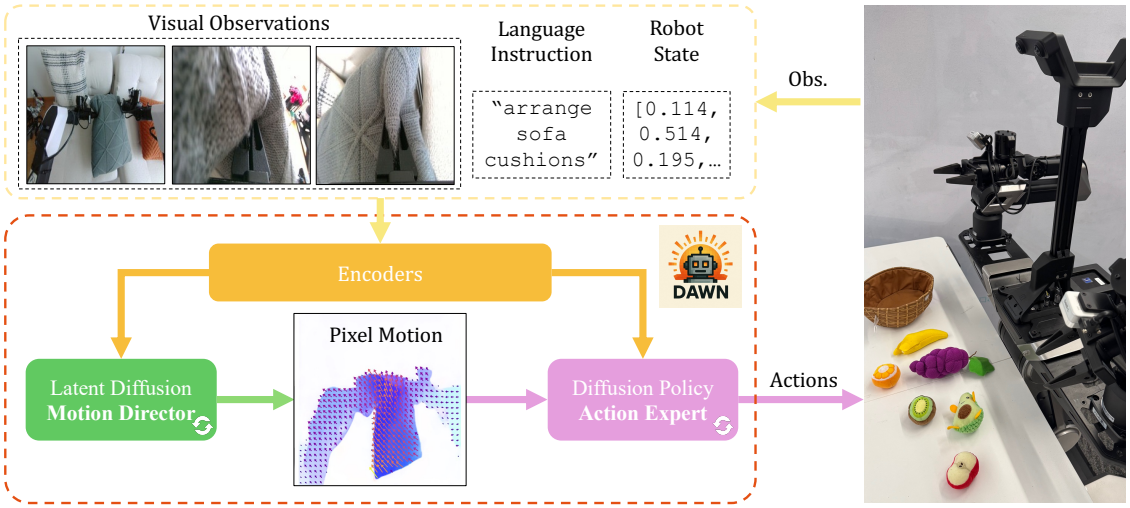

Figure 1. Overview of DAWN with two major diffusion modules. Given visual observations, robot state, and a language instruction, a latent diffusion Motion Director predicts a dense pixel motion representation that describes the desired scene dynamics, which the diffusion policy Action Expert uses to generate executable robot actions. Explicit pixel motion provides a structured, interpretable interface between perception and control.

Abstract

We present DAWN (Diffusion is All We Need for robot control), a unified diffusion-based framework for language-conditioned robotic manipulation that bridges high-level motion intent and low-level robot action via structured pixel motion representation. In DAWN, both the high-level and low-level controllers are modeled as diffusion processes, yielding a fully trainable, end-to-end system with interpretable intermediate motion abstractions. DAWN achieves state-of-the-art results on the challenging CALVIN benchmark, demonstrating strong multi-task performance, and further validates its effectiveness on MetaWorld. Despite the substantial domain gap between simulation and reality and limited real-world data, we demonstrate reliable real-world transfer with only minimal finetuning, illustrating the practical viability of diffusion-based motion abstractions for robotic control. Our results show the effectiveness of combining diffusion modeling with motion-centric representations as a strong baseline for scalable and robust robot learning.

1. Introduction

Recent vision-language-action (VLA) models [5, 6, 16, 19, 49] have achieved strong generalization by leveraging large-scale web and robot datasets. Some works [22, 26, 44, 48, 50] suggest that it is beneficial to include explicit spatial reasoning and motion awareness into the action generation process. Several approaches [2, 3, 12, 43, 46] introduce multi-stage pixel or point tracking to form interpretable intermediate motion cues.

More recently, predictive representations based on video diffusion and GPT-style forecasting models [15, 42] are utilized to predict future observations directly. Gen2Act [2]

*Equal contribution.

extracts motion trajectories by tracking pixels within their generated videos. The motion trajectories offer fine-grained guidance on intended movements, which has been empirically shown to improve robotic control. This insight motivates a simplified approach in which we directly predict dense pixel motions instead of RGB video frames, thereby reducing complexity and making the underlying learning problem easier for the network.

Therefore, we propose **D**iffusion is **A**ll **W**e **N**eed for robot control (DAWN), a two-stage diffusion-based visuomotor framework that predicts *dense pixel motion explicitly* rather than deriving it indirectly from generated videos, detectors, or keypoints. Both the high-level and low-level controllers are implemented as diffusion models and are connected through structured pixel motion, forming an interpretable and modular control pipeline (see Figure 1). Our Motion Director uses a latent diffusion model to generate dense pixel motion fields conditioned on current observations and language instruction. These pixel motions serve as an intermediate representation of desired scene dynamics to accomplish the language instruction. The Action Expert, a diffusion-based policy model, then translates these motions to executable robot actions, forming a coherent control framework. Our approach bridges the strengths of hierarchical motion decomposition and end-to-end visuomotor agents, while maintaining interpretability and modularity.

We evaluate our method on two challenging simulation benchmarks—CALVIN [24] and MetaWorld [45], as well as across real-world environments with only very limited in-domain training data.

Our results demonstrate that, despite using limited data and substantially smaller model capacity, our method can match or even surpass state-of-the-art VLA models by leveraging explicit structured pixel motion and the strengths of diverse pretrained models, highlighting its high data efficiency.

Our key contributions are as follows:

1. We propose DAWN, a two-stage diffusion-based framework that generates structured intermediate pixel motion as an efficient language-conditioned visuomotor policy.
2. Despite relying on limited data and a substantially smaller model capacity, we achieve competitive or even state-of-the-art performance on CALVIN, MetaWorld, and real-world benchmarks.
3. Our approach is explicitly designed to leverage pretrained vision and language models, enabling highly data-efficient transfer across domains, while providing interpretability and modularity.

2. Related Work

Sparse Pixel Trajectories for Robot Control: Several prior works explore pixel trajectories as motion representations [2, 3, 15, 28]. These methods capture the displacement of pixels between consecutive frames, providing a local description of motion that is universal and often embodiment-agnostic. For instance, General Flow [46] proposes a language-conditioned sparse 3D flow prediction model trained on large-scale human videos and treats sparse 3D flow as a foundational affordance, providing a scalable, universal language for describing manipulation. FLIP [12] utilizes a flow-centric generative planning model to synthesize long-horizon plans from language-annotated videos, guiding low-level policies. Im2Flow2Act [43] and Track2Act [3] both use point or object flow as a cross-domain interface, bridging the gap between human videos, simulated data, and real-world robot execution to achieve zero-shot manipulation. Finally, Gen2Act [2] takes a generative approach, first imagining a video of future motion in image pixel space and then conditioning a robot policy on the generated video to enable generalizable manipulation.

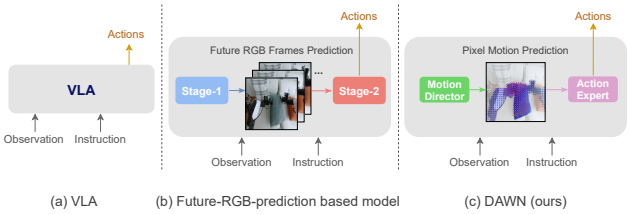

Figure 2. **Comparison of Action-Prediction Frameworks.** a) VLA directly maps observations and language instructions to action outputs. b) Future-RGB-frame-prediction first generate future visual observations and subsequently condition the action policy on these predicted frames. c) Our proposed DAWN predicts pixel-motion representations via the Motion Director and converts them into actions using the Action Expert, enabling a more informative and structured intermediate representation for action prediction.

Pixel trajectories are also found useful when presented in different modalities like image or text. GENIMA [33] fine-tunes a diffusion model to inpaint markers on visual observations, which could be decoded into robot actions. LLaRA [22] presents the robot action in text-based image pixel coordinates and formats the robot policy into a conversation style to benefit from a pretrained large VLM. This enables an efficient transfer from a general VLM into VLA. Similarly, RoboPoint [47], LLARVA [26], TraceVLA [50], Magma [44] and HAMSTER [23] all take advantage of different kinds of textual pixel trajectories.

Unlike these methods that depend on sparse pixel trajectories, our framework predicts high-resolution dense pixel motion during action generation using a latent diffusion model pretrained on general images.

Future RGB Frame Prediction for Robot Control: Recent work has increasingly treated powerful generative video and image models as world models or planners for robot manipulation. SuSIE [4] finetunes an image-editing diffusion model to generate subgoal images from current observations and commands, then realizes it, enabling strong zero-shot generalization. UniPi [11] uses a video-diffusion model to plan future frames from language

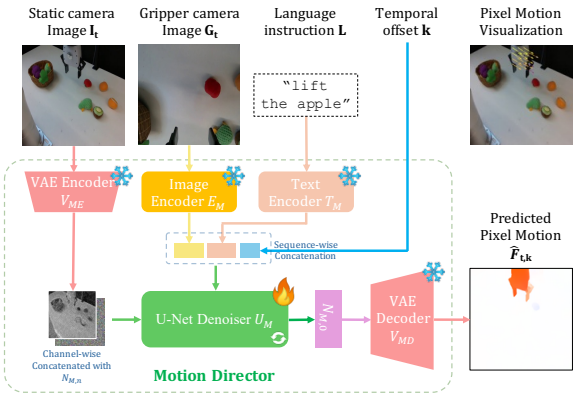

Figure 3. Architecture of Motion Director. The model encodes the static camera view and denoises it with a U-Net, conditioned on the gripper view, language instruction with a temporal offset. The output is decoded into predicted pixel motions, providing interpretable motion representations.

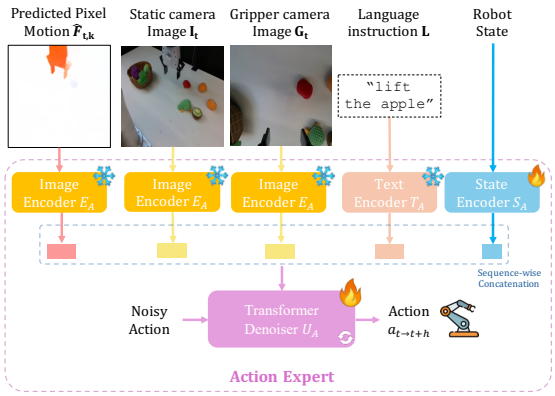

Figure 4. Architecture of Action Expert. The model encodes predicted pixel motion, visual observations, language instruction, and robot state into multimodal features. These inputs condition the denoising process, which iteratively refines noisy actions into executable robot trajectories.

goals and then iinfers actions via inverse dynamics. VidMan [41] pretrains a video-diffusion model on large-scale human data and then adapts it into an inverse-dynamics action model. VPP [15] employs a video diffusion model to extract predictive feature embeddings, which subsequently condition a downstream action policy.

However, these approaches operate purely in RGB space without an explicit motion-centric representation, whereas our method directly predicts dense pixel motion (see Figure 2).

Vision-Language-Action Models: Vision-language-action models have emerged as a powerful paradigm for language-conditioned robot control [1, 7, 8, 10, 17, 19, 27, 29, 37, 42, 44, 48, 50]. Leveraging large-scale training with web-scale vision-language data, these models increasingly focus on improving generalization and data efficiency.

RT-2 [7] jointly finetuned a vision–language model on robot trajectory data and large-scale web image/text tasks. The key idea was to treat robot actions as discrete tokens in the same vocabulary as language tokens, thus enabling a unified modelling framework. OpenVLA [19] continued the discrete-token formulation of actions and emphasized parameter-efficient fine-tuning for new robot setups. π series [6, 16] allows higher fidelity, higher-frequency control with the help of the flow-matching based action expert.

3. Method

3.1. Preliminaries: Diffusion Models

Diffusion models [13, 35, 36] are powerful generative models that synthesize data by iteratively denoising noise-corrupted inputs to approximate the target data distribution. The process involves a forward step that gradually perturbs real data with noise through a Markov chain, and a reverse step in which a neural network parameterizes Gaussian transitions to progressively remove noise, eventually generating realistic samples from a simple distribution such as a standard Gaussian. These models have shown remarkable success in image generation and broader data generation tasks. To improve scalability and efficiency for image generation, latent diffusion models [31] operate in a compressed latent space rather than raw pixel space, significantly reducing computational demands while preserving fidelity.

Diffusion-based approaches have also been adapted for robot learning, where policy learning can be framed as a sequence generation problem. Diffusion Policy [9], in particular, addresses the challenge of visuomotor control by generating action sequences conditioned on both visual and low-dimensional states.

3.2. Problem Formulation and DAWN Overview

We study the topic of language-instructed visuomotor control, where the goal is to build a policy that takes both visual observations and natural language instructions from the environment to generate robot actions for control, using behavior cloning (i.e., supervised learning).

Our approach, DAWN, combines the strengths of two complementary diffusion models: a latent image diffusion model for pixel-level motion generation, referred to as *Motion Director*, and a diffusion transformer for fine-grained action sequence generation, referred to as *Action Expert*. These two models interact through explicit pixel-motion representations. At a higher level, Motion Director conditions on multi-view images and the language instruction to iteratively generate task-aligned pixel motions, grounded to one of the input views as illustrated at Figure 3. At the lower level, Action Expert takes the generated pixel motion along with additional inputs to produce the final robot action sequence as illustrated at Figure 4. We highlight how our pixel-motions are grounded to an input view, endowing our intermediate representations with interpretability.

3.3. Motion Director

Consider two videos $\mathbf{I}, \mathbf{G} \in \mathbb{R}^{T \times H \times W \times C}$ capturing the same robot demonstration from different camera views, each consisting of T frames of height H, width W, and C channels, along with the corresponding language instruction $\mathbf{L}$. For example, $\mathbf{I}$ could be the video from a static third-person view, and $\mathbf{G}$ could be captured from the camera above the gripper. Let $\mathbf{I}_t, \mathbf{G}_t$ denote the t-th frame from the corresponding views. We define the pixel motion from $\mathbf{I}_t$ to $\mathbf{I}_{t+k}$ as $\mathbf{F}_{t,k} = [u, v]$, where $u, v \in \mathbb{R}^{H \times W}$ represent amount of movement of each pixel between $\mathbf{I}_t$ and $\mathbf{I}_{t+k}$ in the horizontal and vertical directions, respectively. To take advantage of pretrained models, we further encode this motion into a three-channel image $\mathbf{F'}_{t,k} = [u, v, (u+v)/2]$.

The goal of Motion Director is to estimate $\mathbf{F'}_{t,k}$ using only current visual input $\mathbf{I}_t$, $\mathbf{G}_t$ and instruction $\mathbf{L}$. Our Motion Director builds on a pretrained latent diffusion model for RGB image generation, comprising a U-Net denoiser U_M, a text encoder T_M, and pretrained VAE encoder–decoder pair (V_{ME}, V_{MD}). We also incorporate a vision encoder E_M to extract embeddings from alternative camera views.

At the inference time, we first draw a Gaussian noise $\mathbf{N}_{M,n}$ and concatenate it with the latent encoding of the current frame $V_{ME}(\mathbf{I}_t)$, forming a noisy latent representation $\mathbf{O}_{M,n} = [N_{M,n}, V_{ME}(\mathbf{I}_t)]$, where n is the total number of denoising steps we plan to execute. Note that the current frame latent encoding $V_{ME}(\mathbf{I}_t)$ does not undergo any form of corruption, as this is a conditioning signal. The U-Net U_M then denoises $\mathbf{O}_{M,n}$ and outputs a less noisy latent $N_{M,n-1}$ under the conditioning of the language embedding $T_M(\mathbf{L})$, visual embedding of the alternative view $E_M(\mathbf{G}_t)$, and a temporal offset k. All conditioning tokens are concatenated and injected into the U-Net's cross-attention layers at each denoising step. The denoised latent tensor will be concatenated again with the VAE encoded visual inputs to form the input for the next denoising step $\mathbf{O}_{M,n-1} = [N_{M,n-1}, V_{ME}(\mathbf{I}_t)]$. For an arbitrary denoising step i, the process can be presented as below, where t_i is the denoising timestamp and [...] stands for concatenation.

$$\mathbf{O}_{M,i} = [N_{M,n}, V_{ME}(\mathbf{I}_t)] \tag{1}$$

$$\mathbf{C}_M = [E_M(\mathbf{G}_t), T_M(\mathbf{L}), k] \tag{2}$$

$$\mathbf{N}_{M,i-1} = U_M(\mathbf{O}_{M,i}, \mathbf{C}_M, t_i) \tag{3}$$

After n iterations, the denoised latent tensor $\mathbf{N}_{M,0}$ is decoded by V_{MD} into a three-channel image, which ideally matches the ground-truth motion $\mathbf{F'}_{t,k}$.

During training, we update only the U-Net denoiser U_M, while keeping all other modules frozen. The ground-truth pixel motion corresponding to frame $\mathbf{I}_t$ is obtained using the optical flow model RAFT [38] since we have access to future frames during training (i.e., using frames $\mathbf{I}_t$ and $\mathbf{I}_{t+k}$ as input to RAFT), and subsequently projected into latent space through the VAE encoder V_{ME}.

3.4. Action Expert

Our Action Expert is responsible for translating pixel motions into low-level robot actions, conditioned on visual observations, robot states, and language instructions. To achieve this, motivated by prior diffusion based policies [9], we construct a transformer based Enhanced Diffusion Policy, which generates action sequences by progressively denoising noisy action representations under multimodal conditions. This design enables the policy to capture complex dependencies across modalities while producing coherent actions temporally.

The architecture consists of four key components: (1) a shared visual encoder V_A that encodes both the pixel motion output from Motion Director and the current visual observations, (2) a text encoder T_A that embeds the language instruction, (3) a state encoder S_A that processes low-dimensional robot states through a two-layer MLP, and (4) a denoising transformer U_A that generates action sequences. We initialize U_A and S_A from scratch to allow adaptation to the target task, while keeping the pretrained V_A and T_A frozen to benefit from strong pretrained visual and language representations.

During inference, the pixel motion predicted by Motion Director, together with the visual inputs, language instruction, and robot states, are each processed by their corresponding encoder and projected into token embeddings. These context tokens are concatenated to form the conditioning sequence, which is injected into all transformer blocks of the denoising transformer U_A via cross-attention, following the same mechanism as in Motion Director. Action generation begins from a noisy action chunk with length h sampled from a Gaussian prior, which is iteratively denoised by U_A into a coherent sequence of executable robot actions.

3.5. DAWN Training and Inference

In summary, both Motion Director and Action Expert are trained with a mean squared error noise estimation loss. While Motion Director operates in the latent image space to predict pixel motions, Action Expert focuses on predicting action chunks in the robot's action space.

At inference, observations are first encoded, after which Motion Director produces a single pixel-motion field that conditions Action Expert to generate a sequence of robot actions. Once these actions are executed, the system repeats the process with the updated observations, thereby forming a closed-loop control pipeline.

One advantage of this design is that the two diffusion models can be trained in parallel using the optical flow between two images as the ground-truth pixel motion. Two modules could be upgraded independently, enabling flexible integration of future advances in vision or control. After that, Action Expert could optionally be further fine-tuned on the actual pixel motions generated by Motion Director

for a better performance.

To the best of our knowledge, this is the first work to adapt a pretrained *latent* diffusion model for dense pixel *motion* generation and use the pixel motion to guide a diffusion policy for visuomotor control under fully learnable settings.

4. Experiments

We evaluate our framework on two challenging simulation benchmarks—CALVIN [24] and MetaWorld [45], as well as across real-world environments involving diverse robotic manipulation tasks. In this section, we first introduce our experimental setup, followed by evaluations on the three selected robotics environments, and finally ablation studies.

4.1. Implementation Details

Our DAWN comprises two components, Motion Director and Action Expert. We initialize our Motion Director from a pretrained latent diffusion model from [31, 32] that has been trained on large-scale image-text datasets. The additional U-Net weights we use for our additional visual conditioning are zero-initialized to ensure that the pretrained network behavior is preserved at the beginning of training, and the model can gradually adapt to the additional input modality. We encode the language instruction and extract gripper view visual tokens using CLIP model. During the inference, we use 25 diffusion steps to generate the final pixel motion prediction.

Our Action Expert conditions on visual, textual, and robotic state modalities with different encoders for each input. The visual encoder is a pretrained ConvNeXt-S variant of DINOv3 [34], and the text encoder is a T5-small pretrained model.

4.2. CALVIN Experiments

Dataset: We first evaluate our DAWN on the CALVIN benchmark [24]. This simulated benchmark measures the long-horizon capability of robotic manipulation tasks. We focus on the most challenging ABC→D task setting, where the model is trained on the A, B, and C environments and then evaluated in the unseen D environment. We follow standard evaluation protocol from [15, 42]. More details is provided in Supplementary Materials.

Results: We report results under two training settings, first without using any external robotic demonstration data in Table 1 and second with external robotic demonstration data (DROID) in Table 2. Since we follow evaluation protocol identical to [15, 28], baseline results in our tables are directly borrowed from these prior works.

In Table 1, our DAWN achieves state-of-the-art results, highlighting the promise of pixel-motion based representations for complex robotic manipulation tasks. We also report results for our only the low-level Action Expert as Enhanced DP. These results highlight the clear impact of pixel motions in achieving the strong results of our overall DAWN framework. Example rollouts are presented in the appendix.

In the case of using external robotic data, direct comparison to prior works (where different approaches use different pretraining data) is less straightforward. We report results for our DAWN that is trained jointly on the DROID dataset and CALVIN ABC→D split. Our DAWN outperforms several recent works and performs competitively against SOTA methods VPP [15] and DreamVLA [49]. In Table 2, VPP benefits from significantly more videos (including 193k human manipulation trajectories, 179k robot manipulation trajectories, CALVIN, MetaWorld, and additional real-world datasets) in its pretraining. Similarly, DreamVLA was first pretrained on a language-free split of the CALVIN and the full DROID dataset.

Overall, our DAWN achieves state-of-the-art performance on CALVIN benchmark, demonstrating the scalability as well as strong data efficiency of intermediate pixel-motion based VLA approaches.

4.3. Meta-World Experiments

Dataset: We next evaluate DAWN on the MetaWorld [45] simulated environment containing a Sawyer robot arm. We focus on 11 challenging tasks constructed following [20, 28] since the original benchmark is not language conditioned. We use the training split from [20, 28] containing 165 actionless videos for Motion Director training and 220 task demonstrations across the 11 tasks for Action Expert training. All baseline experiments and results are identical to those reported in prior works AVDC [20] and LTM [28].

Results: We report these results in Table 3. Our approach achieves clear performance improvements compared to prior works on this challenging benchmark. We particularly emphasize the improved *semantic understanding* of our DAWN framework: notice how DAWN achieves significantly better performance on visually similar but semantically dissimilar task pairs such as `open-door` vs `close-door`. We attribute this to our efficient latent diffusion formulation that enables scalable language-video pretraining, which in turn endows our model with stronger language understanding. We also highlight the improved performance in tasks such as `basketball` and `assembly`, which we attribute to our action-expert design choices that enable better robot state awareness.

4.4. Real-world Single-arm Manipulation

We set up our single-arm environment with a 7-DoF xArm7 robot arm and two RGB cameras: one providing a fixed third-person view from the right side of the arm, and the other mounted above the gripper (see Figure 5). A dataset of 1000 episodes is then collected, comprising lift-and-place manipulations involving six types of toys and a container.

Implementation: We compare our approach against three strong baselines. The first is our modification of Diffusion

Table 1. **CALVIN Evaluation (no external robotic data):** Results reported for zero-shot long-horizon evaluation on the Calvin ABC→D benchmark. All methods are trained only on the CALVIN dataset without any external data.

Method	i^{th} Task Success Rate					Avg. Len ↑
	1	2	3	4	5	
Diffusion Policy [9]	0.40	0.12	0.03	0.01	0.00	0.56
Robo-Flamingo [21]	0.82	0.62	0.47	0.33	0.24	2.47
MoDE [30]	0.92	0.79	0.67	0.56	0.45	3.39
RoboUniview [44]	0.94	0.84	0.73	0.62	0.51	3.65
Seer [39]	0.93	0.82	0.72	0.63	0.53	3.64
Seer-Large [39]	0.93	0.85	0.76	0.69	0.60	3.83
VPP [15]	0.96	0.88	0.78	0.71	0.60	3.93
Enhanced DP (ours)	0.82	0.67	0.53	0.41	0.35	2.78
DAWN (ours)	0.98	0.91	0.79	0.71	0.61	4.00

Table 2. **CALVIN Evaluation with external robotic data:** Zero-shot long-horizon evaluation on the Calvin ABC→D benchmark where agent is asked to complete five chained tasks sequentially based on instructions.

Method	Additional Data	i^{th} Task Success Rate					Avg. Len ↑
		1	2	3	4	5	
GR-1 [42]	Ego4D	0.85	0.71	0.60	0.50	0.40	3.06
Vidman [41]	OpenX subsets	0.92	0.76	0.68	0.59	0.47	3.42
LTM [28]	OpenX subsets	0.97	0.82	0.73	0.67	0.61	3.81
Seer [39]	DROID	0.94	0.87	0.80	0.72	0.64	3.98
MoDE [30]	Multiple sources	0.96	0.89	0.81	0.72	0.65	4.01
Seer-Large [39]	DROID	0.96	0.92	0.86	0.80	0.74	4.28
VPP [15]	Multiple sources	0.97	0.91	0.87	0.82	0.77	4.33
DreamVLA [49]	DROID	0.98	0.95	0.90	0.83	0.78	4.44
DAWN (ours)	DROID	0.98	0.92	0.81	0.75	0.64	4.10

Table 3. **MetaWorld task success rate:** Our DAWN achieves state-of-the-art performance on MetaWorld.

Method	*door-open*	*door-close*	*basketball*	*shelf-place*	*btn-press*	*btn-top*	*faucet-close*	*faucet-open*	*handle-press*	*hammer*	*assembly*	*Overall*
BC-Scratch [25]	21.3	36.0	0.0	0.0	34.7	12.0	18.7	17.3	37.3	0.0	1.3	16.2
BC-R3M [25]	1.3	58.7	0.0	0.0	36.0	4.0	18.7	22.7	28.0	0.0	0.0	15.4
Diffusion Policy	45.3	45.3	8.0	0.0	40.0	18.7	22.7	58.7	21.3	4.0	1.3	24.1
UniPi [11] (With Replan)	0.0	36.0	0.0	0.0	6.7	0.0	4.0	9.3	13.3	4.0	0.0	6.1
Im2Flow2Act [43]	0.0	0.0	0.0	4.0	6.3	0.0	7.3	4.7	0.0	0.0	0.0	2.0
ATM [40]	75.3	90.7	24.0	16.3	77.3	76.7	50.0	62.7	92.3	4.3	2.0	52.0
AVDC [20] (Flow)	0.0	0.0	0.0	0.0	1.3	40.0	42.7	0.0	66.7	0.0	0.0	13.7
AVDC [20] (Default)	72.0	89.3	37.3	18.7	60.0	24.0	53.3	24.0	81.3	8.0	6.7	43.1
LTM [28]	77.3	95.0	39.0	20.3	82.7	84.3	52.3	68.3	98.0	10.3	7.7	57.7
DAWN (ours)	94.7	97.3	42.0	24.7	92.0	91.7	76.3	79.0	98.0	12.7	10.7	65.4

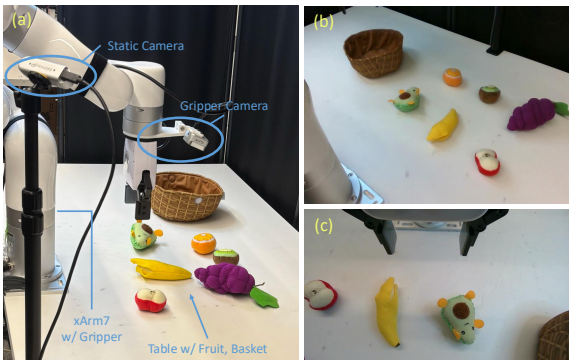

Figure 5. **Real-world environment examples.** a) Our single-arm environment includes a robot arm and two cameras. They are stereo RGB cameras, but we only use one RGB view from each camera. b) The RGB image from the static camera. c) The RGB image from the gripper camera.

Policy [9], Enhanced DP, which is identical to our Action Expert but without pixel motion from a Motion Director. This model is pretrained on CALVIN ABC dataset. The second baseline is π_0 [6], where we initialize from the π_0 base model and apply Low-Rank Adaptation (LoRA) [14]. The third is VPP [15], initialized from their official pre-trained checkpoint. All methods are fine-tuned on our collected real-world dataset for 100k steps. The task is highly challenging for the policy to learn, as a total of only 1k episodes across 12 tasks provides very limited training data.

Evaluation: We evaluate all methods using the lift-and-place task pair with different objects, where the robot is instructed to lift a specified object and place it into a container. We record the number of episodes in which the robot: (i) successfully lifts the correct object, (ii) successfully places the correct object, (iii) lifts an incorrect object at the end with 500 max steps, and (iv) places the incorrect object from the previous lifting. Note that (iii) and (iv) are still classified as failures, though they differ from complete failures to grasp or place the object. We include these cases to provide a clearer understanding of the failure patterns. Each episode begins from a randomly initialized environment, and we run 20 episodes per task in total.

Results: Table 4 shows that DAWN achieves the highest success rates across nearly all object categories, outperforming π_0, VPP, and Enhanced DP. Compared to π_0 and VPP, DAWN exhibits better semantic grounding and more consistent lifting of the correct object. Figure 6 illustrates a representative failure case for π_0, contrasted with a successful trajectory from DAWN. The Enhanced DP baseline

Table 4. **Real-world single lift-and-place evaluation**. For each task, we evaluate 20 episodes with random initialization position.

	Apple		Avocado		Banana		Grape		Kiwi		Orange		Inference
	Success ↑ (i)→(ii)	Wrong Obj. ↓ (iii)→(iv)	Success ↑ (i)→(ii)	Wrong Obj. ↓ (iii)→(iv)	Success ↑ (i)→(ii)	Wrong Obj. ↓ (iii)→(iv)	Success ↑ (i)→(ii)	Wrong Obj. ↓ (iii)→(iv)	Success ↑ (i)→(ii)	Wrong Obj. ↓ (iii)→(iv)	Success ↑ (i)→(ii)	Wrong Obj. ↓ (iii)→(iv)	**Efficiency (ms)** ↓
Enhanced DP	5→4	9→8	6→6	6→4	5→4	6→4	4→3	8→6	5→5	6→5	4→4	8→7	112.77
π_0 [6]	10→9	9→9	6→6	12→10	5→3	11→6	8→5	10→8	5→3	12→12	8→7	11→11	571.89
VPP [15]	16→14	2→2	15→15	2→0	15→14	0→0	17→17	1→0	15→15	2→0	16→14	0→0	190.55
DAWN	**19→19**	0→0	**20→19**	0→0	**17→16**	0→0	**19→19**	0→0	**17→16**	2→2	**18→16**	0→0	319.82

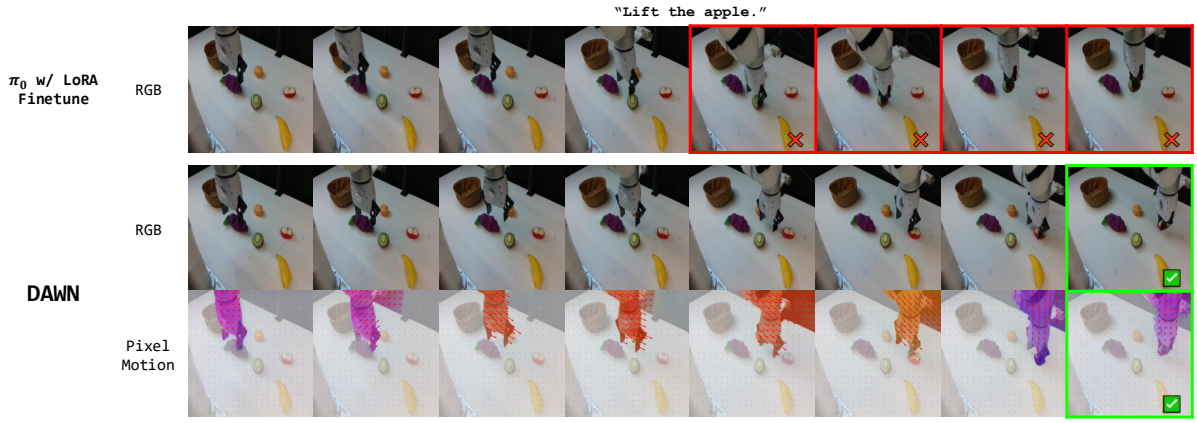

Figure 6. **Real world rollout examples**. For "lift the apple," π_0 lifts the wrong object (top), while DAWN succeeds in the same setting (middle). Pixel motion predicted by Motion Director is shown in the last row.

Method	MSE↓
Enhanced Diffusion Policy	0.128
Ours	0.117

Table 5. **Bimanual manipulation results.** Mean squared error (MSE) of action prediction on the test set. Our approach achieves lower error compared to the baseline.

(without pixel motion) frequently grasps the wrong object, demonstrating that structured pixel motion from Motion Director provides complementary benefits and can further strengthen even strong two-stage diffusion based methods such as VPP.

Efficiency: We report the average inference runtime for each chunk of action steps in the last column of Table 4. Enhanced DP is the fastest baseline since it uses a single diffusion model without any additional high-level module. VPP is slightly slower but remains efficient because its video diffusion model operates in a single forward pass to extract predictive features, without explicitly generating video frames or pixel-level outputs. DAWN has higher computational time due to its two-stage design: the Motion Director first predicts explicit pixel motion and the Action Expert then produces actions conditioned on this motion. Despite the overhead, DAWN still runs at practical closed-loop frequencies and achieves the highest overall success rates, indicating that the benefits of explicit motion reasoning outweigh the added inference time.

4.5. Bimanual Manipulation

We further extend our framework in a more challenging bimanual setting using the Galaxea R1-Lite. The setup includes two 7-DoF arms with a gripper, a head static camera, and two wrist-mounted cameras. Similarly, though the cameras are stereo cameras, we only use a single RGB frame from each camera for our experiments.

Implementation and Evaluation: We train our model on the subset of Galaxea Open-World Dataset [18]. The subset contains more than 100 hours of real-world demos, covering nine different types of challenging bimanual tasks in seven real-world environments.

We report the mean squared error (MSE) of predicted joint actions on a test set of 300 episodes. We compare our proposed model against the baseline Enhanced Diffusion Policy (without pixel motion from Motion Director), as shown in Table 5. Results show that our approach achieves consistently lower MSE, indicating that structured pixel motion improves the accuracy of action prediction even in the more complex bimanual setting. Figure 7 shows two example samples from the test set where DAWN can predict the correct pixel motion corresponding to the given observations. These findings suggest that the benefits of our two-stage framework generalize beyond single-arm tasks and extend to multi-arm coordination scenarios.

4.6. Ablation Study

We conduct ablation experiments on the CALVIN ABC→D benchmark to assess the impact of (a) structured pixel mo-

Figure 7. **Galaxea pixel motion prediction examples**. The first column shows the one test image sequence given the task of "arrange sofa cushions". The second column shows the test image sequence given the task of "chair push and place". Each group shows the original head-camera observation and the visualizations of corresponding pixel motions predicted by Motion Director.

Table 6. Ablation study on CALVIN dataset.

Setting	Avg. Length
(a) Pixel Motion vs RGB Goal	
None	2.78
RGB Goal	3.21
Pixel Motion w/o pretrained	3.42
Pixel Motion	**4.00**
(b) Gripper View	
VPP w/o gripper view	3.58
DAWN w/o Gripper view	3.74
DAWN w/ Gripper View	**4.00**
(c) # of Diffusion steps of Motion Director	
2	3.88
10	3.96
25	**4.00**
40	3.95

tion representation, (b) gripper view conditioning, and (c) the number of diffusion steps (See Table 6).

(a) Pixel Motion, RGB Goal, and pretraining. We compare two variants against our default setting: (i) RGB goal image conditioning instead of pixel motion; (ii) Only Action Expert w/o pixel motion, and (iii) generating pixel motion with a denoising U-Net trained from scratch. As shown in Table 6 (a), pixel motion yields the best performance, highlighting its utility as a structured and interpretable intermediate, and our method benefits a lot from the pretrained image generation model, even though the model was not trained for pixel motion generation before.

(b) Gripper View Conditioning. We further ablate the effect of adding egocentric gripper-mounted observation to Motion Director. Removing the gripper view leads to performance degradation (3.74 vs. 4.00), while prior methods such as VPP degrade further (3.58). These results confirm that the additional viewpoint facilitates reasoning about occlusions and fine-grained hand-object interactions.

(c) Diffusion Steps of Motion Director. Motion Director module can capture meaningful motion information even at 2 diffusion steps (3.88). Increasing the number of steps steadily improves performance, peaking at 25 (4.00) and can't gain more beyond that (e.g., 40 steps with 3.95).

5. Conclusion

In this work, we present a two-stage diffusion-based visuomotor framework for robot manipulation, termed DAWN, which achieves state-of-the-art performance on CALVIN, MetaWorld, and real-world benchmarks. Instead of using manifest visual information in RGB space, we use explicit dense pixel motion representations as a structured interface between a latent diffusion Motion Director and a diffusion-based Action Expert. This design bridges hierarchical motion decomposition and end-to-end agents while preserving interpretability and modularity. By instantiating both stages with modern diffusion models and leveraging strong pre-trained vision language backbones, DAWN delivers high data efficiency and robust transfer, indicating that much of the gap between multi-stage tracking pipelines and VLA/latent-feature hierarchies stems not from the framework itself but from underpowered high- and low-level components. We hope DAWN encourages re-examining structured intermediate representations as a practical path to interpretable, data-efficient robot control.

Acknoledgements

This research was financially supported by the Ministry of Trade, Industry, and Energy (MOTIE), Korea, under the "Global Industrial Technology Cooperation Center(GITCC) program" supervised by the Korea Institute for Advancement of Technology (KIAT).(Task No. P0028420). This research was supported by the National Research Council of Science & Technology(NST) grant by the Korea government(MSIT) (No. GTL25041-000).

References

[1] Shikhar Bahl, Abhinav Gupta, and Deepak Pathak. Human-to-robot imitation in the wild. In *RSS*, 2022.

[2] Homanga Bharadhwaj, Debidatta Dwibedi, Abhinav Gupta, Shubham Tulsiani, and et al. Gen2act: Human video generation in novel scenarios enables generalizable robot manipulation. *arXiv:2409.16283*, 2024.

[3] Homanga Bharadhwaj, Roozbeh Mottaghi, Abhinav Gupta, and Shubham Tulsiani. Track2act: Predicting point tracks from internet videos enables diverse zero-shot robot manipulation. *arXiv:2405.01527*, 2024.

[4] Kevin Black, Mitsuhiko Nakamoto, Pranav Atreya, Homer Rich Walke, and et al. Zero-shot robotic manipulation with pretrained image-editing diffusion models. *arXiv:2310.10639*, 2023.

[5] Kevin Black, Noah Brown, Danny Driess, Adnan Esmail, and et al. $pi0$: A vision-language-action flow model for general robot control. *arXiv:2410.24164*, 2024.

[6] Kevin Black, Noah Brown, Danny Driess, Adnan Esmail, and et al. pi_0: A vision-language-action flow model for general robot control. *arXiv:2410.24164*, 2024.

[7] Anthony Brohan and et al. RT-2: Vision-language-action models transfer web knowledge to robotic control. *arXiv:2307.15818*, 2023.

[8] Anthony Brohan, Noah Brown, Justice Carbajal, Yevgen Chebotar, and et al. RT-1: Robotics transformer for real-world control at scale. *RSS*, 2023.

[9] Cheng Chi, Siyuan Feng, Yilun Du, Zhenjia Xu, and et al. Diffusion policy: Visuomotor policy learning via action diffusion. *arXiv:2303.04137*, 2023.

[10] Danny Driess, Fei Xia, Mehdi SM Sajjadi, Corey Lynch, and et al. Palm-e: An embodied multimodal language model. *arXiv:2303.03378*, 2023.

[11] Yilun Du, Mengjiao Yang, and et al. Learning universal policies via text-guided video generation, 2023.

[12] Chongkai Gao, Haozhuo Zhang, Zhixuan Xu, Zhehao Cai, and Lin Shao. Flip: Flow-centric generative planning as general-purpose manipulation world model, 2024.

[13] Jonathan Ho, Ajay Jain, and Pieter Abbeel. Denoising diffusion probabilistic models. *NeurIPS*, 33:6840–6851, 2020.

[14] Edward J Hu, Yelong Shen, Phillip Wallis, Zeyuan Allen-Zhu, and et al. Lora: Low-rank adaptation of large language models. *ICLR*, 2022.

[15] Yucheng Hu, Yanjiang Guo, Pengchao Wang, Xiaoyu Chen, and et al. Video prediction policy: A generalist robot policy with predictive visual representations. *arXiv:2412.14803*, 2024.

[16] Physical Intelligence, Kevin Black, Noah Brown, James Darpinian, Karan Dhabalia, and et al. $pi0.5$: a vision-language-action model with open-world generalization, 2025.

[17] Youngjoon Jeong, Junha Chun, Soonwoo Cha, and Taesup Kim. Object-centric world model for language-guided manipulation. *arXiv:2503.06170*, 2025.

[18] Tao Jiang, Tianyuan Yuan, Yicheng Liu, Chenhao Lu, Jianning Cui, Xiao Liu, Shuiqi Cheng, Jiyang Gao, Huazhe Xu, and Hang Zhao. Galaxea open-world dataset and g0 dual-system vla model. *arXiv preprint arXiv:2509.00576*, 2025.

[19] Moo Jin Kim, Karl Pertsch, Siddharth Karamcheti, Ted Xiao, and et al. Openvla: An open-source vision-language-action model. *arXiv:2406.09246*, 2024.

[20] Po-Chen Ko, Jiayuan Mao, Yilun Du, Shao-Hua Sun, and Josh Tenenbaum. Learning to act from actionless videos through dense correspondences. *arXiv:2310.08576*, 2023.

[21] Xinghang Li, Minghuan Liu, Hanbo Zhang, Cunjun Yu, and et al. Vision-language foundation models as effective robot imitators. *arXiv:2311.01378*, 2023.

[22] Xiang Li, Cristina Mata, Jong Sung Park, Kanchana Ranasinghe, and et al. Llara: Supercharging robot learning data for vision-language policy. *arXiv:2406.20095*, 2024.

[23] Yi Li, Yuquan Deng, Jesse Zhang, Joel Jang, Marius Memmel, Raymond Yu, Caelan Reed Garrett, Fabio Ramos, Dieter Fox, Anqi Li, et al. Hamster: Hierarchical action models for open-world robot manipulation. *arXiv preprint arXiv:2502.05485*, 2025.

[24] Oier Mees, Lukas Hermann, Erick Rosete-Beas, and Wolfram Burgard. Calvin: A benchmark for language-conditioned policy learning for long-horizon robot manipulation tasks. *RAL*, 7(3):7327–7334, 2022.

[25] Suraj Nair, Aravind Rajeswaran, , and et al. R3m: A universal visual representation for robot manipulation, 2022.

[26] Dantong Niu, Yuvan Sharma, Giscard Biamby, Jerome Quenum, and et al. Llarva: Vision-action instruction tuning enhances robot learning. *arXiv:2406.11815*, 2024.

[27] Abhishek Padalkar and et al. Open x-embodiment: Robotic learning datasets and rt-x models. *arXiv:2310.08864*, 2023.

[28] Kanchana Ranasinghe, Xiang Li, Cristina Mata, Jong Sung Park, and et al. Pixel motion as universal representation for robot control. *arXiv:2505.07817*, 2025.

[29] Scott Reed, Konrad Zolna, Emilio Parisotto, Sergio Gomez Colmenarejo, and et al. A generalist agent. In *TMLR*, 2022.

[30] Moritz Reuss, Jyothish Pari, Pulkit Agrawal, and Rudolf Lioutikov. Efficient diffusion transformer policies with mixture of expert denoisers for multitask learning. In *The Thirteenth International Conference on Learning Representations*, 2025.

[31] Robin Rombach, Andreas Blattmann, Dominik Lorenz, Patrick Esser, and Björn Ommer. High-resolution image synthesis with latent diffusion models. In *CVPR*, pages 10684–10695, 2022.

[32] Robin Rombach, Andreas Blattmann, Dominik Lorenz, Patrick Esser, and Björn Ommer. Stable diffusion v1.5 (model card), 2025.

[33] Mohit Shridhar, Yat Long Lo, and Stephen James. Generative image as action models. *arXiv:2407.07875*, 2024.

[34] Oriane Siméoni, Huy V Vo, Maximilian Seitzer, Federico Baldassarre, and et al. Dinov3. *arXiv:2508.10104*, 2025.

[35] Jascha Sohl-Dickstein, Eric Weiss, Niru Maheswaranathan, and Surya Ganguli. Deep unsupervised learning using nonequilibrium thermodynamics. In *ICML*, pages 2256–2265. PMLR, 2015.

[36] Jiaming Song, Chenlin Meng, and Stefano Ermon. Denoising diffusion implicit models. In *ICLR*, 2021.

[37] Sruthi Sudhakar, Ruoshi Liu, Basile Van Hoorick, Carl Vondrick, and et al. Controlling the world by sleight of hand. *arXiv:2408.07147*, 2024.

[38] Zachary Teed and Jia Deng. Raft: Recurrent all-pairs field transforms for optical flow. In *ECCV*, pages 402–419, 2020.

[39] Yang Tian, Sizhe Yang, Jia Zeng, Ping Wang, and et al. Predictive inverse dynamics models are scalable learners for robotic manipulation. *arXiv:2412.15109*, 2024.

[40] Chuan Wen, Xingyu Lin, John So, Kai Chen, and et al. Any-point trajectory modeling for policy learning. *arXiv:2401.00025*, 2023.

[41] Youpeng Wen, Junfan Lin, Yi Zhu, Jianhua Han, and Xiaodan Liang. Vidman: Exploiting implicit dynamics from video diffusion model for effective robot manipulation. *NeurIPS*, 37:41051–41075, 2024.

[42] Hongtao Wu, Ya Jing, Chilam Cheang, Guangzeng Chen, and et al. Unleashing large-scale video generative pre-training for visual robot manipulation. *arXiv:2312.13139*, 2023.

[43] Mengda Xu, Zhenjia Xu, Yinghao Xu, Cheng Chi, and et al. Flow as the cross-domain manipulation interface. *arXiv:2407.15208*, 2024.

[44] Jianwei Yang, Reuben Tan, Qianhui Wu, Ruijie Zheng, and et al. Magma: A foundation model for multimodal ai agents. In *CVPR*, pages 14203–14214, 2025.

[45] Tianhe Yu, Deirdre Quillen, Zhanpeng He, Ryan Julian, and et al. Meta-World: A Benchmark and Evaluation for Multi-Task and Meta Reinforcement Learning. In *CoRL*, 2019.

[46] Chengbo Yuan, Chuan Wen, Tong Zhang, and Yang Gao. General flow as foundation affordance for scalable robot learning. *arXiv:2401.11439*, 2024.

[47] Wentao Yuan, Jiafei Duan, Valts Blukis, Wilbert Pumacay, and et al. Robopoint: A vision-language model for spatial affordance prediction for robotics. *arXiv:2406.10721*, 2024.

[48] Michal Zawalski, William Chen, Karl Pertsch, Oier Mees, and et al. Robotic control via embodied chain-of-thought reasoning. In *CoRL*, 2024.

[49] Wenyao Zhang, Hongsi Liu, Zekun Qi, Yunnan Wang, and et al. Dreamvla: A vision-language-action model dreamed with comprehensive world knowledge. *arXiv:2507.04447*, 2025.

[50] Ruijie Zheng, Yongyuan Liang, Shuaiyi Huang, Jianfeng Gao, and et al. Tracevla: Visual trace prompting enhances spatial-temporal awareness for generalist robotic policies. *arXiv:2412.10345*, 2024.

Pixel Motion Diffusion is What We Need for Robot Control

Supplementary Material

1. Training Details

We train all models on a single node with 4 NVIDIA A6000 GPUs. For Motion Director, we train for 100k iterations with a per-GPU batch size of 16. For Action Expert, we train for 10k iterations with a per-GPU batch size of 64. We use the AdamW optimizer with a learning rate of 1×10^{-4}. Mixed precision training is used to reduce memory usage and improve throughput. All training is implemented in PyTorch with the HuggingFace Diffusers and Transformers libraries.

2. Dataset details

2.1. CALVIN

Dataset: CALVIN is an open source simulated benchmark to learn long-horizon language-conditioned tasks, which contains 4 different simulation environments-A, B, C, D. While each split (A–D) shares the same robotic setup, variations in object placement, textures, lighting, and distractors ensure that models cannot rely on memorization but must instead demonstrate robust visuomotor understanding. The 34 manipulation tasks span a wide range of skills such as pushing, placing, rotating, toggling switches, and opening drawers, all expressed through natural language instructions.

Evaluation: We follow standard evaluation protocol from [15], which evaluates a given policy on 1000 episodes each containing 5 continuous tasks (i.e. task i starts from the end state of task $i-1$, which is often different to what is encountered in demonstrations within the training data). For each task, at most 360 action steps are performed unless the task is successfully completed prior to that. The success rate for each consecutive task is averaged across the 1000 episodes and reported. Considering the 5 continuous tasks as a sequences, the average number of tasks completed by the policy (i.e. average length) is also reported.

2.2. DROID

DROID is a large-scale "in-the-wild" robot manipulation dataset featuring 76k real demonstration trajectories across 564 varied scenes and 86 tasks. It provides over 350 hours of interaction data, with diverse viewpoints, object types, and natural instruction annotations.

2.3. Real World

2.3.1. xArm Environment

We constructed a dataset specifically for fine-tuning and real-world evaluation. The experimental platform consists of a 7-DoF xArm7 manipulator and two RGB cameras. An Intel RealSense D435 was positioned laterally to provide a third-person view of the workspace, while an Intel RealSense D405 was mounted above the gripper to capture a close-up view of the end-effector and its interactions with objects. Though both cameras are stereo cameras, we only use a single RGB view from each camera in all the experiments. This dual-camera setup enables complementary perspectives, facilitating both scene-level and fine-grained observations.

Data was collected through a leader–follower teleoperation scheme, where a human operator controlled a leader device to guide the motions of the xArm7 (follower). Each demonstration episode was restricted to a single atomic task, such as lifting a fruit, transporting it, or placing it into a basket. Episodes were initialized either from randomized joint configurations or from the terminal state of the preceding task, ensuring diversity in initial conditions. To further increase variability and promote generalization, we occasionally re-dropped and re-grasped objects within the same episode.

The resulting dataset comprises 1,000 episodes, with a minimum of 100 demonstrations allocated to each distinct task. This distribution ensures both task balance and sufficient coverage for downstream fine-tuning. Overall, the dataset provides a structured yet diverse collection of manipulation trajectories suitable for evaluating task-specific policies under realistic conditions.

2.3.2. Galaxea R1 Lite Environment

In order to evaluate on more complicated environment, we also constructed a dataset for fine-tuning and real-world evaluation. This environment contains a bi-manual Galaxea R1 Lite platform and three RGB cameras. A RGB camera was positioned medially to provide the head view of the workspace, while the other two Intel Realsense D405 was mounted above two grippers in each side to capture the close-up view of the end-effector and their interactions with objects. Though both of the gripper-view cameras are stereo cameras, we only use a single RGB view from each camera in all the experiments.

We set up a table top manipulation environment, which has two plush toys: a lion and an elephant, also a toy pot. In terms of the tasks, we are manipulating plush toys and the lid cover of the toy pot (one hand manipulates a plush toy, and the other hand helps open the lid cover of the toy pot). See Figure 10 for the example and Table 7 for the task description.

We collected our data through a leader-follower teleoperation scheme, which human operates the Galaxea R1 Lite Teleop to guide the motions of the Galaxea R1 Lite (follower). Each demonstration episode was a single bi-manual

Task	Language
left_place_lion	left arm lift and place lion into pot, right arm helps open and close lid.
left_place_elephant	left arm lift and place elephant into pot, right arm helps open and close lid.
left_pick_lion	left arm pick lion from pot, right arm helps open and close lid.
left_pick_elephant	left arm pick elephant from pot, right arm helps open and close lid.
right_place_lion	right arm lift and place lion into pot, left arm helps open and close lid.
right_place_elephant	right arm lift and place elephant into pot, left arm helps open and close lid.
right_pick_lion	right arm pick lion from pot, left arm helps open and close lid.
right_pick_elephant	right arm pick elephant from pot, left arm helps open and close lid.

Table 7. Task definitions used in our Galaxea Real World experiments.

pick-place task, such as picking the lion into the pot and helping to open the lid. The collected dataset comprises 150 episodes, which provides a structured collection of learnable bi-manual manipulation trajectories.

3. Qualitative Results

This section includes a series of visualizations demonstrating how DAWN generates and executes pixel-motion plans across diverse environments. All videos and overlays are packaged locally and can be viewed through the provided index.html together with this supplementary.

3.1. Bi-manual Pixel Motion Predictions

We first showcase Motion Director's pixel-motion predictions on bimanual manipulation sequences. These include both our own recorded bimanual setup and Galaxea-Open-World-Dataset videos. In each case, we overlay the predicted pixel motion on each frame to reveal how the Motion Director captures coordinated left–right arm movements, object-relative displacements, and long-range motion cues. These examples highlight that the motion plans remain consistent even in visually complex or asymmetric dual-arm settings. Our two examples of Galaxea-Open-World-Dataset pixel motion prediction are presented in Figure 9. Another two examples of our real world environment pixel motion prediction are presented in Figure 10.

3.2. Real-World xArm Manipulation

Next, we provide full rollout videos from our real-world xArm7 platform (see Figure 8). For every rollout, we include third-person view and frame-by-frame pixel-motion overlays. These visualizations show that the robot's actual behavior reliably follows the predicted motion. This makes the high-level plan interpretable, which is one of the key advantages of using structured pixel-motion as the intermediate representation.

3.3. CALVIN Rollout

We also include additional CALVIN rollout examples with paired RGB frames and predicted pixel motions. Similar to the real-world experiments, Motion Director produces clean, directional pixel-motion fields, and Action Expert executes them through temporally coherent low-level actions. These long-horizon sequences further confirm the consistency between planned and executed motion, even when the tasks involve multi-object interactions, distractors, or ambiguous scene layouts. Our two example rollouts are presented in Figure 11.

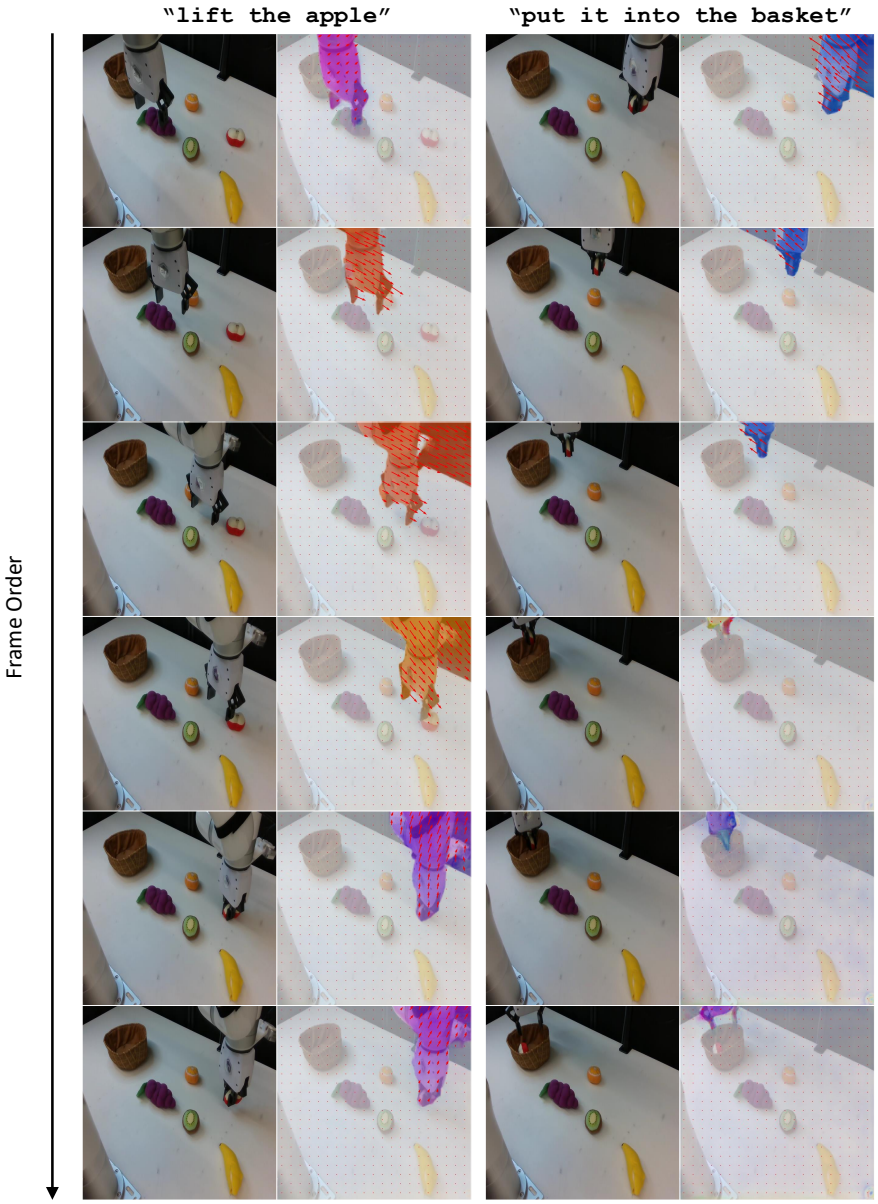

Figure 8. **xArm rollout examples**. The first column shows the observation sequence given the task of "lift the apple". The second column shows the observation sequence given the task of "put it into the basket". Each group shows the original static-camera observation and the visualizations of corresponding pixel motions predicted by Motion Director.

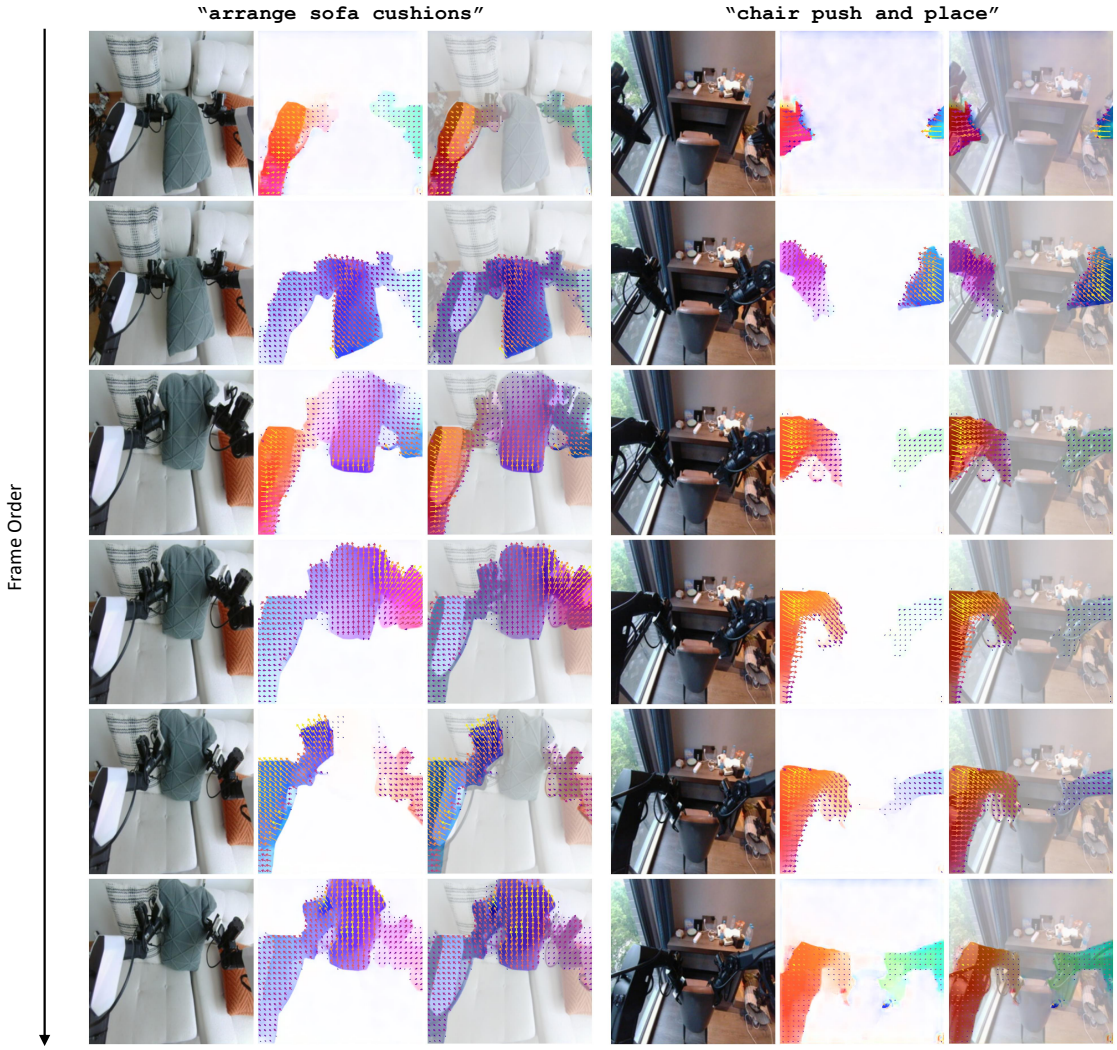

Figure 9. **Galaxea-Open-World-Dataset pixel motion prediction examples**. The first column shows the one test image sequence given the task of "arrange sofa cushions". The second column shows the test image sequence given the task of "chair push and place". Each group shows the original head-camera observation and the visualizations of corresponding pixel motions predicted by Motion Director.

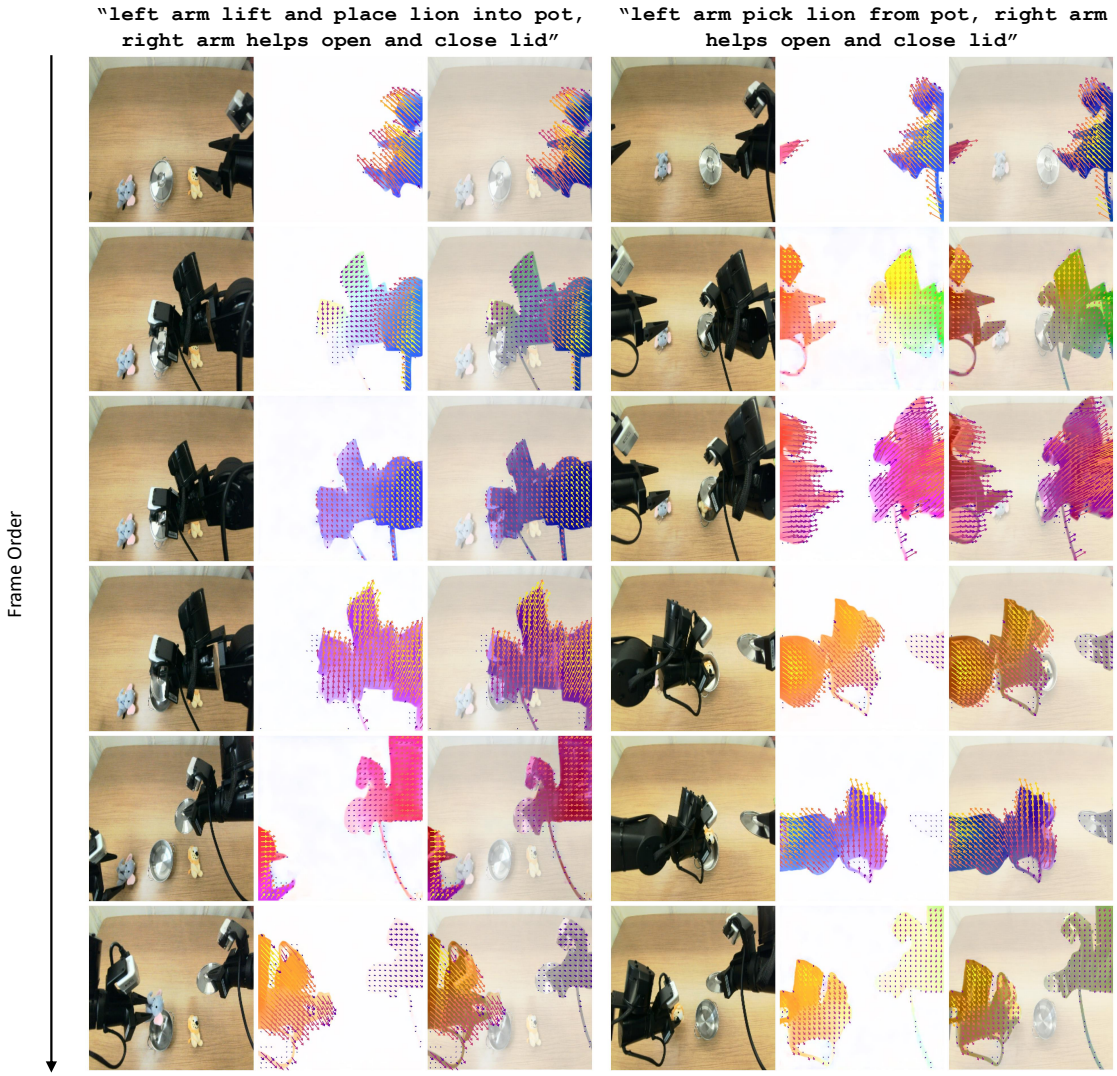

Figure 10. **Real-World Galaxea pixel motion prediction examples**. The first column shows the one test image sequence given the task of "left arm lift and place lion into pot, right arm helps open and close lid". The second column shows the test image sequence given the task of "left arm pick lion from pot, right arm helps open and close lid". Each group shows the original head-camera observation and the visualizations of corresponding pixel motions predicted by Motion Director.

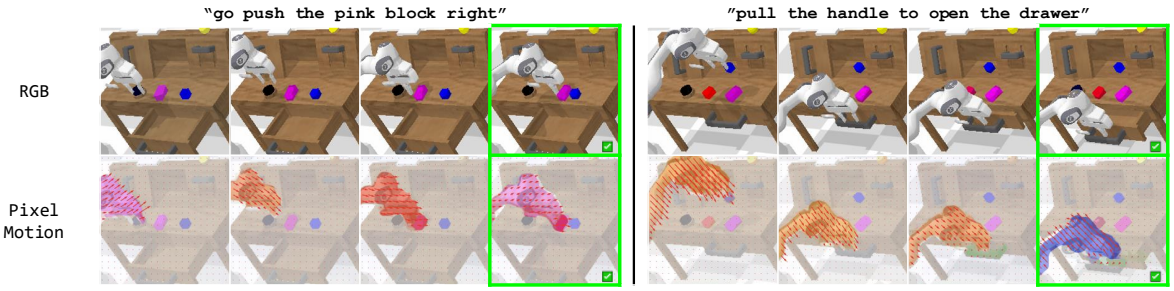

Figure 11. **CALVIN rollout examples**. Two example rollouts of DAWN in CALVIN environment. The first row is the sequence of RGB images, and the second row is the visualization of the corresponding pixel motions predicted by Motion Director.